

## Magnetic Imaging of Superconducting Tapes to Determine Current Flow

G.W. Brown<sup>a</sup>, M.E. Hawley<sup>a</sup>, S.R. Foltyn<sup>b</sup>, and F.M. Mueller<sup>b</sup>

<sup>a</sup>Structure/Property Relations (MST-8),

<sup>b</sup>Superconductivity Technology Center (MST-STC),

Materials Science & Technology Division,

Los Alamos National Laboratory, Los Alamos, NM 87545

### ABSTRACT

We have developed a magnetic imaging system that uses magnetoresistive read heads from computer hard disk drives to map the transport-current-induced magnetic field at the surface of superconducting tapes at liquid nitrogen temperature. Transport current pathways are determined from the 2-dimensional magnetic field maps using established inversion schemes. We examined the current flow in pulsed-laser-deposited  $\text{YBa}_2\text{Cu}_3\text{O}_{7-\delta}$  films patterned on single crystal  $\text{SrTiO}_3$  substrates and on a textured yttria-stabilized-zirconia layer deposited on an Inconel ribbon by ion beam assisted deposition. The transport current densities in all cases were consistent with the Critical State Model. For the Inconel-based sample, the transport current density maps have allowed us to observe defects and determine the region that limits the current carrying capacity of the structure.

### INTRODUCTION

A variety of electrical power applications could be improved by replacing conventional conductors with superconductors operating at liquid nitrogen temperature.  $\text{YBa}_2\text{Cu}_3\text{O}_{7-\delta}$  films on metal tape substrates are promising candidates for these applications because of the large  $J_c$  (and  $I_c$ ) attainable at liquid nitrogen temperatures over moderate lengths of material.<sup>1</sup> In order to produce longer YBCO coated conductors, current limiting defects must be eliminated, since even one region of low  $J_c$  limits the performance of the entire tape. It is therefore important to be able to map the transport current to see where these regions of low critical current density are located.

To address this need, we have developed an imaging apparatus capable of mapping the normal component of the transport-current-induced magnetic field at the surface of a superconducting sample at 75 K (immersed in liquid nitrogen).<sup>2</sup> Our sensors are magnetoresistive devices scanned over the surface of the sample, making this a type of scanning magnetoresistance microscopy<sup>3</sup>. The magnetic field maps are numerically inverted, using the Biot-Savart law, to provide the spatial dependence of the transport current density  $J$ . These maps are useful since they reveal the current paths under conditions similar to those encountered in actual use.

Mapping transport current by measuring and inverting the self-field has previously been applied to superconducting samples using either magneto-optical imaging<sup>4,5</sup> or scanning Hall probe instruments.<sup>6,7</sup> Our implementation combines the benefits of negligible sample preparation, very little sensor preparation, flexible imaging conditions, high resolution data, and straightforward sensor response.

## EXPERIMENTAL

We obtain magnetic field maps by scanning a magnetic sensor over the sample surface. A schematic of the instrument is shown in Fig. 1a. The sample and sensor are immersed in liquid nitrogen during the experiment. The sensor is attached to a brass strip mounted at the bottom of a scan rod. The end of the rod protruding from the dewar is rastered by a high resolution x-y scanner. A fixed pivot point near the sample translates the scanner motion into sensor motion and reduces the total travel by about a factor of 5. Before scanning, the pivot rod is lowered towards the sample so that the tension in the brass strip keeps the sensor in contact with the sample surface. For the data shown here, 50  $\mu\text{m}$  of Kapton plastic was inserted between the sensor and sample to prevent sample damage during raster motion. This also fixes the sensor-sample spacing. Even with this protection layer, however, the sliding motion generates about 7 G equivalent noise on the sensor signal. Scratches are also visible on the plastic after each experiment. Voltage maps acquired from the head are converted to magnetic field maps by calibrating against sources with known magnetic field strength.

The sensors are permalloy-based magnetoresistive read-heads fabricated for use in computer hard disk drives by a commercial manufacturer.<sup>8</sup> The active area of the heads is less than  $1 \mu\text{m}^2$  and room temperature sensitivities are typically better than  $3 \mu\text{V/G}$ . Measurements at liquid nitrogen temperature show a sensitivity of  $> 1 \mu\text{V/G}$  with a linear response measured up to 250 G when used in a constant current mode. The geometry of the heads makes them sensitive to the surface normal component of the magnetic field.

Current density maps are obtained from the magnetic field maps by inverting the Biot-Savart law using established Fourier space techniques.<sup>9</sup> The film thickness is assumed to be infinitesimal (since 50  $\mu\text{m}$  is a large sensor-sample separation) and high frequency Fourier component noise is filtered with a sharp cutoff. Similar methods were used to invert the self-field data in the studies noted above. Because of the large sensor-sample separation, we expect the image resolution to be  $\sim 50 \mu\text{m}$ . To facilitate inversion, images were acquired as  $2^n \times 2^n$  pixel maps. Before inversion, the images were mirrored about the  $x$ - and  $y$ - axes to create a supercell without offsets at the image edges.

The samples for this work were YBCO deposited by pulsed laser deposition under typical conditions<sup>1</sup> and patterned into bridges. Two types of substrate were used –  $\text{SrTiO}_3$  and textured YSZ on Inconel ribbon. Sample “A” was YBCO deposited on single crystal  $\text{SrTiO}_3$ . In order to achieve an  $I_c$  near 10 A, 300 nm of YBCO was deposited and patterned into a bridge 1 mm wide and 5 mm long. The measured  $I_c$  of sample A was 10 A ( $J_c = 3.4 \times 10^6 \text{ A/cm}^2$ ). Sample “B” was fabricated by depositing 600 nm of YBCO on a textured YSZ layer previously deposited by ion beam assisted deposition on an Inconel ribbon. This was then patterned into a bridge structure 1 mm wide and 7 mm long. The thickness and width were chosen to provide  $I_c$  near 10 A on this substrate based on previous experience, however, the measured value was only 6 A ( $J_c = 1 \times 10^6 \text{ A/cm}^2$ ), indicating some defect present in the sample.

For imaging, the fast scan direction of the raster motion was perpendicular to the bridge length (the main transport current direction). The typical imaging orientation and coordinate axes used for discussion are shown in Fig. 1b. The only data smoothing applied was a small vertical adjustment of adjacent scan lines to remove offsets. The typical imaging time for the data was about 45 minutes. The current density maps we present will show only the  $x$ -component of the current density (that flowing along the bridge length) since there is very little current flowing across these particular samples.

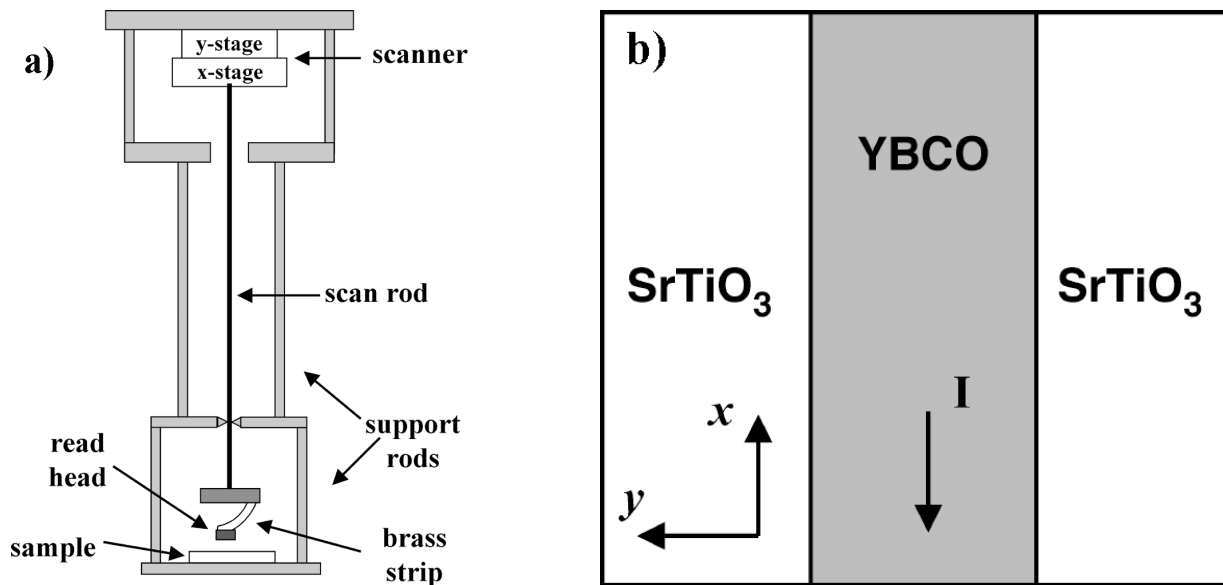


Figure 1: a) Schematic diagram of the apparatus used for imaging the magnetic field at the surface of the superconducting device. b) Schematic diagram of the typical bridge orientation, size, current flow direction and coordinate axes relative to the images shown below.

## RESULTS AND DISCUSSION

### Sample A

The magnetic field map of sample A with 6 A flowing is shown in Fig. 2a. In the gray scale image it is possible to see the light and dark peaks in magnetic field qualitatively expected from the Biot-Savart law. The  $J_x$  map resulting from inversion of Fig. 2a is shown in Fig 2b and the average line scans from 2a and 2b are shown in Fig. 2c and 2d, respectively. From these panels we see that the current density has a doubly peaked structure with the maxima near the edges of the tape. A small amount of non-uniformity is visible in the gray scale image.

This doubly peaked current density is consistent with the Critical State Model<sup>10</sup> of superconductors applied to thin film geometry<sup>11</sup>. Here, demagnetizing effects change the expected step function current distribution at the sample edges (caused by vortex pinning) to one that has finite current in the center of the sample and current peaks at the edges. In addition, material non-uniformity and instrumental broadening smooth the edge distribution more.

Figures 2e and 2f show  $J_x$  and its 1-dimensional average for the same sample with 12 A flowing in the same direction. These data were acquired soon after the 6 A data and the current was increased monotonically between the two values. Figure 2h shows that the current density has acquired a single peak in the middle of the sample. The gray scale image shows roughly the same amount of non-uniformity in the overall current distribution.

The singly peaked distribution is consistent with the flux-flow state of superconductors, since 12 A is above  $I_c$  for sample A. After a constant current distribution is obtained across the full width of the sample at  $I_c$ , additional current flows down the center of the sample in a

dissipative mode. Similar results above and below the critical current were also seen in a slightly thicker YBCO coating (380 nm).

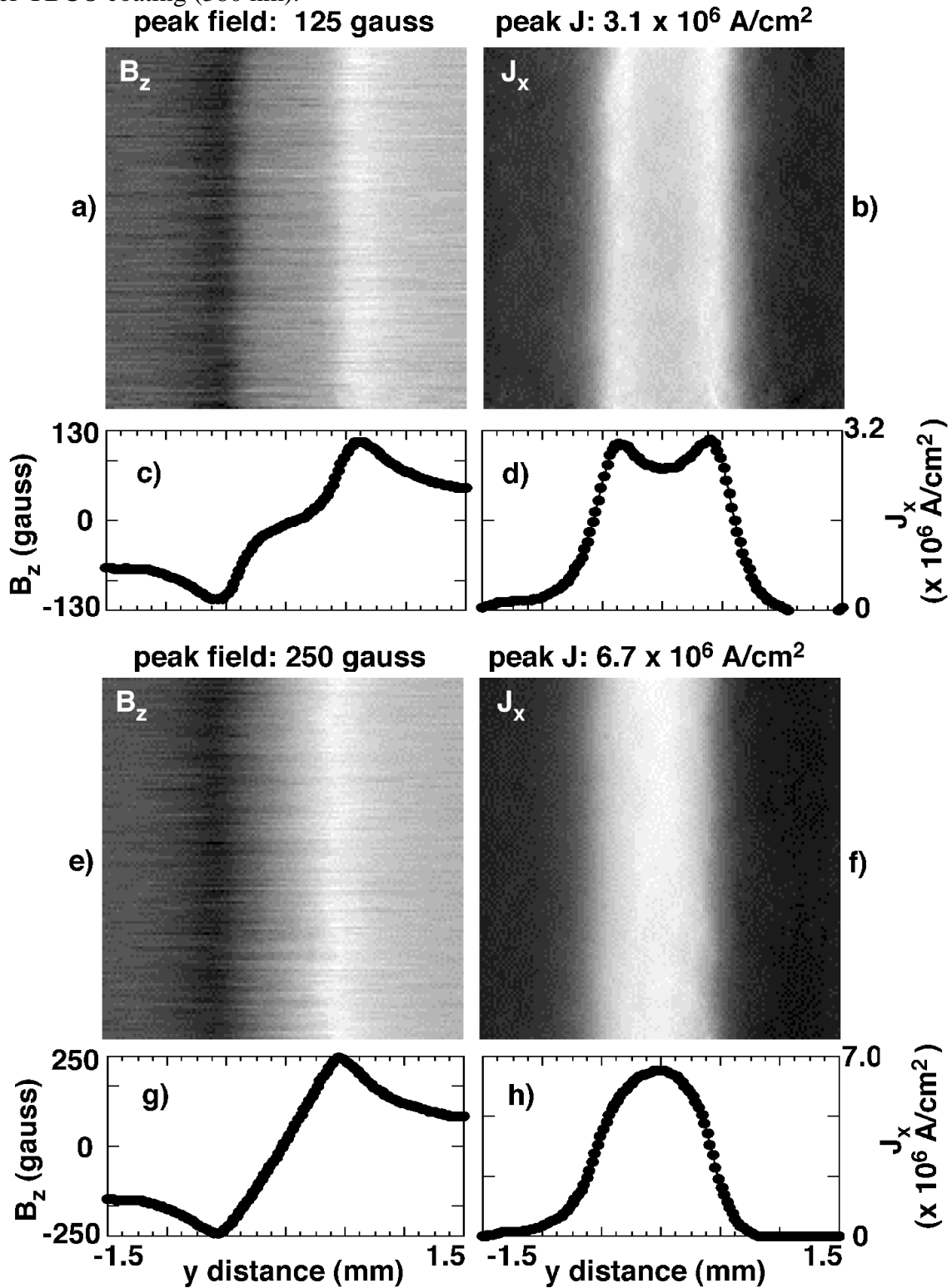


Figure 2: a)  $B_z$  map from sample A carrying 6 Amps. b)  $J_x$  map obtained from inverting panel a). c) average  $B_z$  line scan from sample A carrying 6 Amps. d) average  $J_x$  line from panel b).

e)  $B_z$  map from sample A carrying 12 Amps. f)  $J_x$  map obtained from inverting panel e). g) average  $B_z$  line scan from sample A carrying 12 Amps. h) average  $J_x$  line from panel f).  
**Sample B**

Data from sample B (YSZ/Inconel substrate) are shown in Fig. 3. Figure 3b shows a  $J_x$  map obtained from magnetic field data acquired with 6 A ( $= I_c$ ) flowing. This image covers an area of 3 mm x 9 mm with 64 data points in each horizontal scan line. The images in 3b and 3c are actually made up of three separately acquired images stacked vertically. Slight offsets between them can be seen. From this data, most of the bridge shows the doubly peaked structure similar to those observed on sample A, indicating that most of the device has a critical current greater than 6 A. This is not true of the region slightly below the middle of the bridge which appears to be singly peaked as with the samples in the flux flow state. Since this is the only area on the sample with this type of current density, it must have  $I_c = 6$  A and be the limiting region on this sample. Just below this region, another defect can be seen on the right edge of the bridge. Here, the film has retained a doubly peaked, but narrower structure indicating that  $I < I_c$  in this region and that some other anomaly is constricting the flow to a narrower region. Using AFM we have identified a 750 nm deep crack in the film at this location that is causing the current to move away from the physical edge of the bridge. Further analysis has revealed that this crack appeared when the original 1 cm wide Inconel tape (with textured YSZ coating already deposited) was cut down to 5 mm wide to create the substrate for sample B.

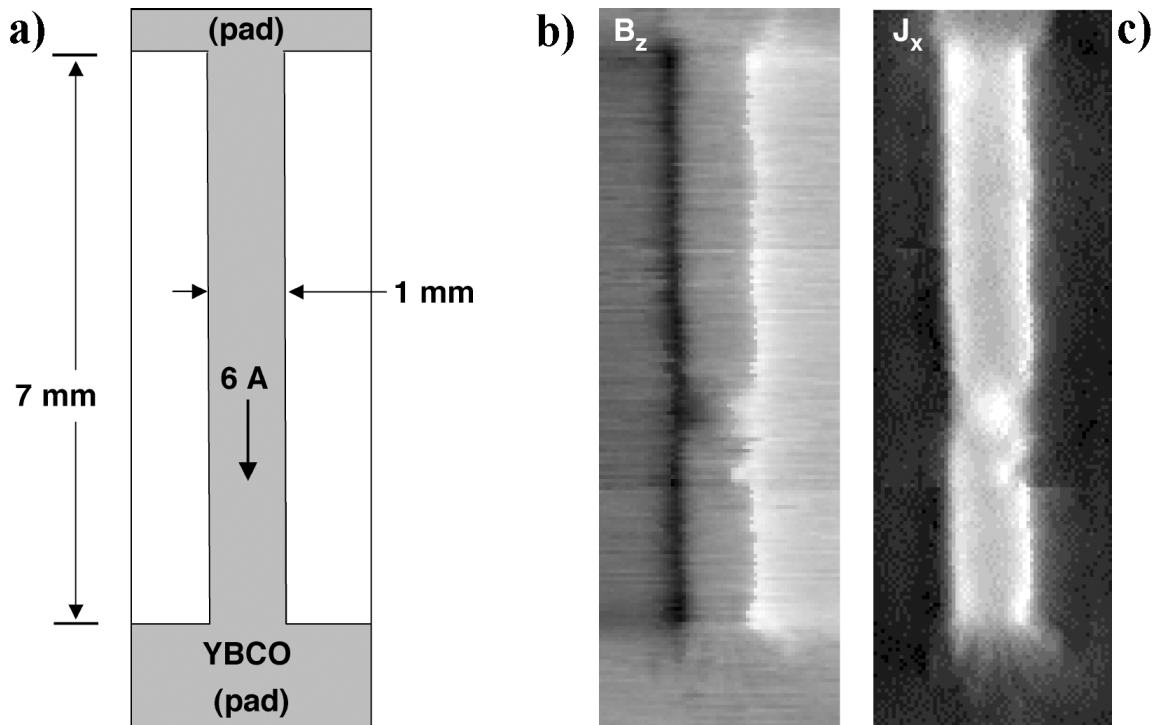


Figure 3: a) schematic diagram of bridge images. b)  $B_z$  map from the YBCO/YSZ/Inconel bridge sample. c)  $J_x$  map from the YBCO/YSZ/Inconel bridge sample.

## Summary and Conclusions

We have developed a low temperature magnetic imaging apparatus that is capable of mapping the self-field of a superconducting sample at 75K. Inverting this data provides a view of the transport current flow in YBCO bridge structures and has allowed us to determine the position and effect of current density defects.

The YBCO/STO sample provided a useful demonstration of the validity of the imaging and inversion processes. The results were completely consistent with the critical state and flux flow state understanding of type II superconductors in thin film form. The data from the YBCO/YSZ/Inconel sample is very promising because, apart from the defects, it shows a high level of similarity to the “ideal” YBCO/STO samples, even though it is prepared in a flexible form that is technologically more useful. Further studies on these kinds of samples should show whether the kinds of defects observed in this work are responsible for the limitations encountered in longer and wider coated conductors.

We thank P. Arendt for assistance with sample growth. We also thank M. Maley for useful discussions on superconductivity and the critical state model. This work was supported by the United States Department of Energy, Office of Energy Efficiency and Renewable Energy.

---

<sup>1</sup> J.O. Willis, et. al., *Physica C* **335**, 73 (2000).

<sup>2</sup> 75 K is the boiling temperature of liquid nitrogen at the altitude of our laboratory in Los Alamos, NM, USA

<sup>3</sup> S.Y. Yamamoto and S. Schultz, *J. Appl. Phys.* **81**, 4696 (1997).

<sup>4</sup> M. Gaevski, A.V. Bobyl, D.V. Shantsev, Y.M. Galperin, T.H. Johansen, M. Baziljevich, H. Bratsberg, and S.F. Karmenko, *Phys. Rev. B* **59**, 9655 (1999).

<sup>5</sup> A.E. Pashitski, A. Palyanskii, A. Gurevich, J.A. Parrell, and D.C. Larbalestier, *Appl. Phys. Lett.* **67**, 2720 (1995).

<sup>6</sup> K. Osamura, K. Matsuno, H. Itoh, T. Horita, H. Tsurumaru, and A. Sakai, *IEEE Trans. Appl. Supercond.* **9**, 2678 (1999).

<sup>7</sup> A. Oota, K. Kawano, and T. Fukunaga, *Physica C* **291**, 188 (1997).

<sup>8</sup> Read-Rite Corp., Milpitas, CA, USA.

<sup>9</sup> B.J. Roth, N.G. Sepulveda, and J.P. Wikswo, Jr., *J. Appl. Phys.* **65**, 361 (1989).

<sup>10</sup> C.P. Bean, *Phys. Rev. Lett.* **8**, 250 (1962).

<sup>11</sup> E. Zeldov, J.R. Clem, M. McElfresh, and M. Darwin, *Phys. Rev. B* **49**, 9802 (1994).